DOI: 10.31534/engmod.2020.1-2.ri.02f
Original scientific paper
Received: 29.03.2019.

Simulation of Human Body Exposure to Near Field of High and Low RF Wireless Power Transfer Systems

Petra Rašić, Maja Škiljo, Zoran Blažević, Vicko Dorić, Dragan Poljak

Department of Electronics and Computing, Faculty of Electrical Engineering, Mechanical Engineering and Naval Architecture, University of Split, Split, Croatia
e-mail: prasic@fesb.hr, mskiljo@fesb.hr, zblaz@fesb.hr, vdoric@fesb.hr, dpoljak@fesb.hr

SUMMARY

In this paper, human body exposure to high frequency electromagnetic field radiated by wireless power transfer system antennas is analysed by numerical modelling using commercial software FEKO. The analysis is carried out for two simplified models of human body (parallelepiped and cylinder model) exposed to high and low frequency radiation in terms of power transfer efficiency and specific absorption rate at frequencies of 13.56 MHz, 6.78 MHz, and 100 kHz. Used simplified models are validated by comparison with realistic human body model results. It is shown in our 5-W power transfer system example that the specific absorption rate in simplified, as well as in realistic, human body model does not exceed the reference limit values prescribed by international guidelines, both for the general and for the professional population. It is also shown that there is no significant difference in specific absorption rate and power transfer efficiency while using different human body models, which is excellent because the theoretical calculations limited on simplified models can be used for human body exposure estimation.

KEY WORDS: *spiral coil; square coil; simplified model of human body; power transfer efficiency; specific absorption rate; wireless power transfer.*

1. INTRODUCTION

Modern people are surrounded by many wireless devices so the question of potential negative influence on human health is a very important one. In addition to this, an increasing number of them rely on wireless charging, a new technology which makes the problem of electromagnetic compatibility even more complicated. In this paper, first, we analyze the interaction between two electrically short antennas (ESAs) in free space at frequencies *f = 13.56 MHz*, *f = 6.78 MHz* and *f = 100 kHz*, in the near field region. These frequencies are assigned radio frequencies (RFs) for industrial, scientific and medical (ISM) use.

The optimum frequency of wireless power transfer (WPT) system operation and various methods for increasing the input resistance and radiation efficiency of ESA are investigated for maximizing the power transfer efficiency (PTE) in WPT systems [1, 2]. For example, the loop with capacitor is used as an indirect, inductive feed for the ESA with no or very small impact on its radiation efficiency at the frequency $f = 13.56\ MHz$ [2]. Decreasing the gap between the driving loop and ESA body, its input resistance can be matched to the required characteristic impedance. The first antenna is transmitting antenna and the second one is receiving antenna initially loaded by $50\ \Omega$. Then, a simplified human body homogenous model with defined relative permittivity and specific conductivity, according to [1], is positioned between these antennas. PTE is analyzed to estimate the influence of the human model on the WPT system performance and on the specific absorption rate (SAR) human exposure to these systems. It is shown herein how the antenna design, the type of human model, distance from the human body model to antenna, and receiver load influence PTE and SAR at low frequencies (LFs) and high frequencies (HFs). The comparison of the simplified and realistic models has been shown in order to estimate the difference between PTE and SAR results which is useful for insight in the use of simplified models and theoretical calculations for interaction between human and WPT systems.

The paper is organized as follows: Some fundamental aspects of human exposure to electromagnetic radiation are given in Section 2; Section 3 depicts a numerical analysis of the interaction between simplified human body models and wireless power systems and comparison with scenarios of realistic human body model. The conclusion is given in Section 4.

2. BIOLOGICAL EFFECTS AND FUNDAMENTAL PRINCIPLES OF ELECTROMAGNETIC RADIATION PROTECTION

The human body is sensitive to HF electromagnetic fields. The exposure to such radiation is quantitatively described by SAR. It is a measure of the rate at which energy is absorbed by the human body when exposed to an RF electromagnetic field. SAR can be averaged either over the *10g* or over the whole body, which is called SAR_{10g} or SAR_{avg}, respectively. SAR is one of the most important parameters of modern dosimetry defined as the time change of energy input *dW* absorbed by the mass element *dm* contained in the volume element *dV* mass density *ρ*:

$$SAR = \frac{dP}{dm} = \frac{d}{dt}\frac{dW}{dm} = \frac{d}{dt}\frac{dW}{dm} = \frac{d}{dt}\frac{dW}{\rho dV} \quad (1)$$

and is expressed in watt per kilogram (*W/kg*) [3]. The storage of electromagnetic energy in a human body and its conversion to heat causes an increase in temperature *T* of the tissue. Therefore, it can also be described by the formula:

$$SAR = C\frac{dT}{dt} \quad (2)$$

where *C* is the specific thermal capacity [2]. In other words, the entire human body becomes a receiving lossy antenna for external high-frequency fields.

Possible damaging effects on human body that may occur when crossing the limits, can be compensated by its own mechanisms (for example shivering, sweating are one of the compensation mechanisms). Therefore, limits to the characteristic parameters of the electromagnetic field to which people may be exposed are prescribed for reducing the risk of possible adverse effects. The most widely accepted international safety guidelines have been issued by International Associations of Non-Ionizing Radiation Protection (ICNIRP); (1998) and Institute of Electrical and Electronics Engineers (IEEE); (1992). They prescribe limit values for electromagnetic fields for the general and professional population, above which people should not be exposed. Most European countries fully comply with the standards prescribed by the ICNIRP guidelines (Table 1). In countries such as the United States and Canada, the guidelines set by IEEE are in place [2].

Table 1. *ICNIRP guidelines for SAR [4]*

Frequency span	*SAR averaged in whole body (W/kg)*	*SAR localized in head and body (W/kg)*	*SAR localized in limbs (W/kg)*
General population			
1 kHz–100 kHz	*0.08*	*2*	*4*
100 kHz–10 MHz	*0.08*	*2*	*4*
10 MHz–10 GHz	*0.08*	*2*	*4*
Professional population			
1 kHz–100 kHz	*0.4*	*10*	*20*
100 kHz–10 MHz	*0.4*	*10*	*20*
10 MHz–10 GHz	*0.4*	*10*	*20*

3. INTERACTION BETWEEN DIFFERENT HUMAN BODY MODELS AND WIRELESS POWER SYSTEMS

3.1 MODELLING OF COILS

The ESA is defined as an antenna whose maximum dimension is less than a 'radianlength' $\lambda/2\pi$ [5] or as the antenna enclosed inside a 'Chu sphere' satisfying the condition $ka < 0.5$ [6], where $k = 2\pi/\lambda$ and a is the radius of a minimum sphere enclosed by the antenna. They generate predominantly the lowest order spherical modes and come close to the concept of the minimum scattering antenna (MSA) [7]. ESAs generally exhibit very small radiation efficiency and input resistance, i.e. small overall efficiency [3, 8]. This is emphasized at lower frequencies due to the dependence of loss and radiation resistance (of TE and TM mode) on frequency as $R^{loss}\sim f^{1/2}$, $R^{TE}\sim f^4$, and $R^{TM}\sim f^2$ respectively [9].

In this section, the simulations are carried out using numerical software FEKO based on Method of Moments (MoM). Homogenous body models require the implementation of sophisticated numerical methods such as Finite Element Method (FEM), which is also used. Realistic body models require the implementation of numerical methods such as Finite Element Method (FEM) [10] – [13], Boundary Element Method (BEM) [14] - [18] or robust methods, such as Finite Difference Time Domain (FDTD) [19]-[22]. Figure 1 shows antennas modeled in FEKO, planar spiral antenna at frequency $f = 13.56$ *MHz* and $f = 100$ *kHz*, and square loops at $f = 6.78$ *MHz* used in standard A4WP specification *1.0* [23]. The coils are made of copper. Different frequency requires a different antenna design. The dimensions of planar spiral antennas are shown in Table 2, where D_{out} is the outer diameter of the coil, D_{in} is the inner diameter of the coil. The free space antenna characteristics at considered frequencies are given in Table 3. For the frequency $f = 13.56$ *MHz* wire segment length is 1 cm, and for the frequency $f = 100$ *kHz* wire segment length is *0.8 cm*. At each frequency, the WPT system consists of two coils. The first coil is transmitting coil with a voltage source of *1 V*, located on port 1. The second coil is receiving one with the load placed on port 2. For frequency $f = 13.56$

MHz the coils are nearly matched to standard *50 Ω* impedance in free space and inductively fed by a loop with a radius of *10.3 cm*, whereas for $f = 6.78$ *MHz* and $f = 100$ *kHz* the antennas are directly fed and not matched (Table 3). The power transfer efficiency PTE is calculated as ratio of the absorbed power by the receiver load R_L and the input transmitter power [24]:

$$PTE = \frac{R_L \left| I_{rx} \right|^2 / 2}{R_{in} \left| I_{tx} \right|^2 / 2} \qquad \textbf{(3)}$$

where R_{in} is input resistance, I_{rx} load current, and I_{tx} current at the input port of the transmitter antenna. PTE at different antenna separations is simulated in the near field using FEKO. The simulations were performed for two receiver load scenarios. The first one is for $Z_L = 50\ \Omega$ with the results depicted in Figures 5, 6 and 7, whereas the second one is the scenario of the optimum matched load $Z_L = Z_{opt}$ ($PTE = PTE_{max}$), shown in Figure 4. It should be noted that Z_{opt} was obtained numerically using the Linville method [24] for each separation between the antennas and every scenario considered. The antennas are placed at the initial separation of $d = 0.01$ *m* and the receiver was separated from the transmitter up to $d = 1.5$ *m*, where the distance d represents the separation between the center of receiving and the center of transmitting antenna. As the receiver moves away from the transmitter, PTE decreases. The conjugate matched load impedance at large enough antenna separations approaches to the impedance of a receiver antenna in free space. Figures 5, 6 and 7 also show that the highest PTE is achieved for the antenna separation $d = 1$ *cm*. For example, at frequency $f = 13.56$ *MHz* PTE_{max} has reached *93 %*. When the receiver separates from the transmitter, it drops, and after $d = 2$ *m* it falls below *5 %* for all the frequencies considered in the simulation.

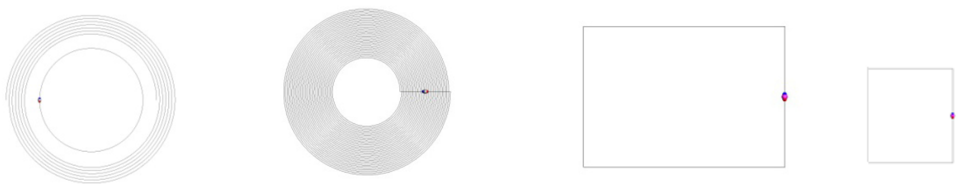

(a) (b) (c) (d)

Fig. 1 *Geometry of planar spiral antenna (a) f = 13.56 MHz, (b) f = 100 kHz and square loop (c) transmitter at f = 6.78 MHz, (d) receiver at f = 6.78 MHz*

Table 2. *Spiral antenna design*

Frequency f (Hz)	D_{out} *(cm)*	D_{in} *(cm)*	*Wire diameter (cm)*	*Number of turns*
13.56 M	*17*	*13*	*0.16*	*6.5*
100 k	*25*	*10*	*0.18*	*30*

Table 3. *Free space characteristics of the simulated antennas*

Frequency f (Hz)	R_{in} *(Ω)*	η_{rad} *(%)*
13.56 M	*54.32*	*2.15*
6.78 M (transmitter)	*0.75*	*0.078*
6.78 M (receiver)	*0.01*	*0.014*
100 k	*0.08*	*0.017*

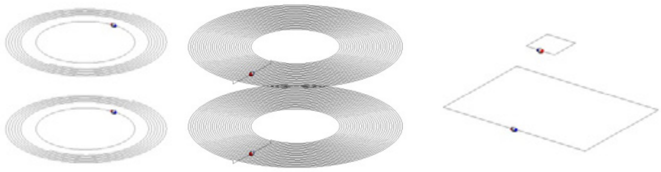

Fig. 2 *Geometry of WPT system on (a) f = 13.56 MHz, (b) f = 100 kHz and (c) f = 6.78 MHz*

3.2 MODELING OF THE HUMAN BODY

In this section, human is exposed to radiation of WPT system consisting of two planar coils placed coaxially to each other at *f = 13.56 MHz*, *f = 6.78 MHz* and *f = 100 kHz* frequencies. The human is modelled as an equivalent parallelepiped, and as an equivalent cylinder with *182 cm x 40 cm x 20 cm* (height (h) x width (w) x depth (d)) dimension, while the interior of the human is represented as a dielectric medium with relative permittivity ε_r and specific conductivity σ, according to Table 4. These parameters are calculated according to [9]. The assumption in paper for equivalent model is that the height and width of the model equal to the height and width of the average human, respectively. Dimensions of the simplified human body models are chosen to correspond to the ones of the realistic human body model. The realistic human is modelled as a homogeneous and isotropic lossy dielectric [2]. The total body model volume for parallelepiped is $0.041\ m^3$ and for cylinder, also, the total volume is $0.041\ m^3$. For realistic model, the total body model volume is $0.052\ m^3$. The receiving antenna is placed behind the back of a human, at a height of *127 cm*, which is the assumption of the worst case, or the highest exposure of humans, as shown in Figure 3 and Figure 4. The antenna parameters are set as in the previous simulation. The analysis is performed for two distances, $d_{human\text{-}transmitter}$ = *20 cm*, and $d_{human\text{-}transmitter}$ = *40.8 cm*, measured from the axis of the model. For calculating SAR_{10g} and SAR_{avg}, the total power delivered to and radiated by the transmitting antenna is always fixed to *5 W* by the conjugate matching procedure. In the case of human presence, the receiving and transmitting antenna is loaded with $Z_L = Z_{opt}$. PTE_{max}, SAR_{10g}, and SAR_{avg} are observed. In the first case, the human is positioned on the distance from the transmitter antenna of $d_{human\text{-}transmitter}$ = *20 cm*, and in the second case, the human is separated from the transmitting antenna $d_{human\text{-}transmitter}$ = *40.8 cm*. For both cases, at the first measurement point, the receiving antenna is located behind the back of the human at the distance of $d_{human\text{-}receiver}$ = *5 cm*, which is the assumption of the worst case scenario.

Table 4. *Characteristics of human muscle tissue at different frequencies [9]*

Frequency f (Hz)	ε_r	*σ (S/m)*
13.56 M	*92*	*0.419*
6.78 M	*210*	*0.391*
100 k	*8020*	*0.362*

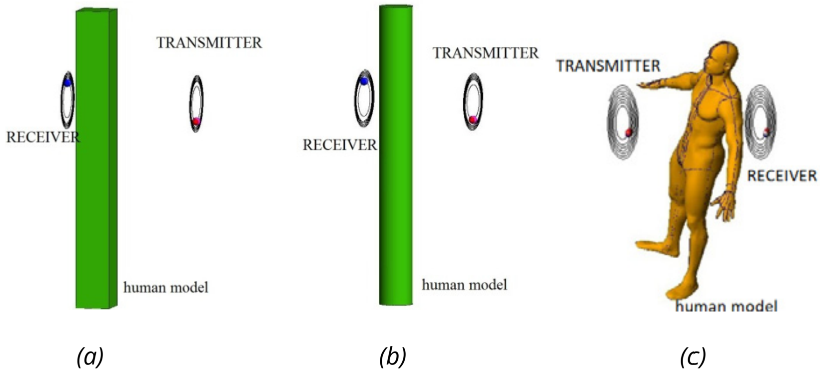

Fig. 3 *Simplified (a) parallelepiped, (b) cylinder human body model and (c) realistic human body model positioned between antennas*

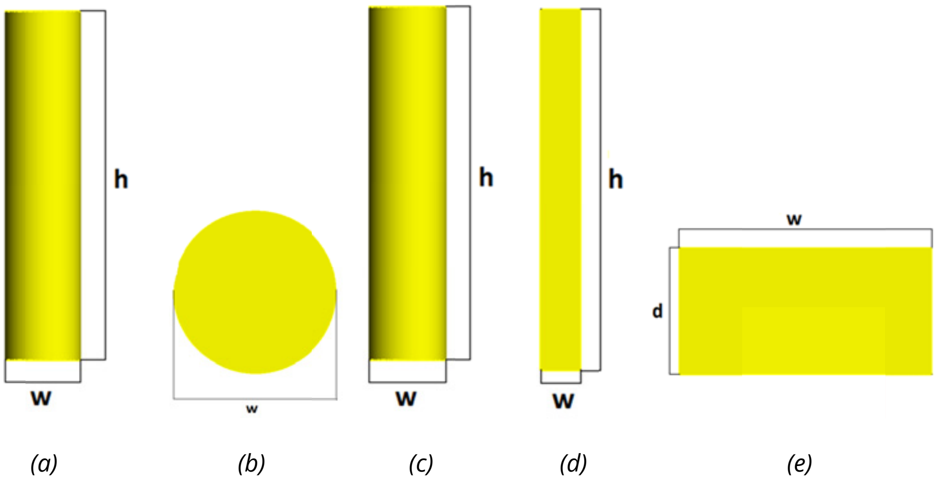

Fig. 4 *Simplified (a) cylinder model (laterally side), (b) cylinder model (top side), (c) parallelepiped model (front side), (d) parallelepiped model (laterally side), (e) cylinder model (top side)*

3.3 SIMULATION OF HUMAN BODY-WPT SYSTEM INTERACTION AND DISCUSSION

In human-WPT system interaction, two parameters are analysed; PTE as estimation parameter for WPT system performance, and SAR to quantify human exposure assessment. Figures 5–13. depict PTE_{max}, SAR_{10g}, and SAR_{avg} in the case of equivalent parallelepiped, cylinder and realistic human body model present in different WPT systems (operating on different frequencies) at given separations.

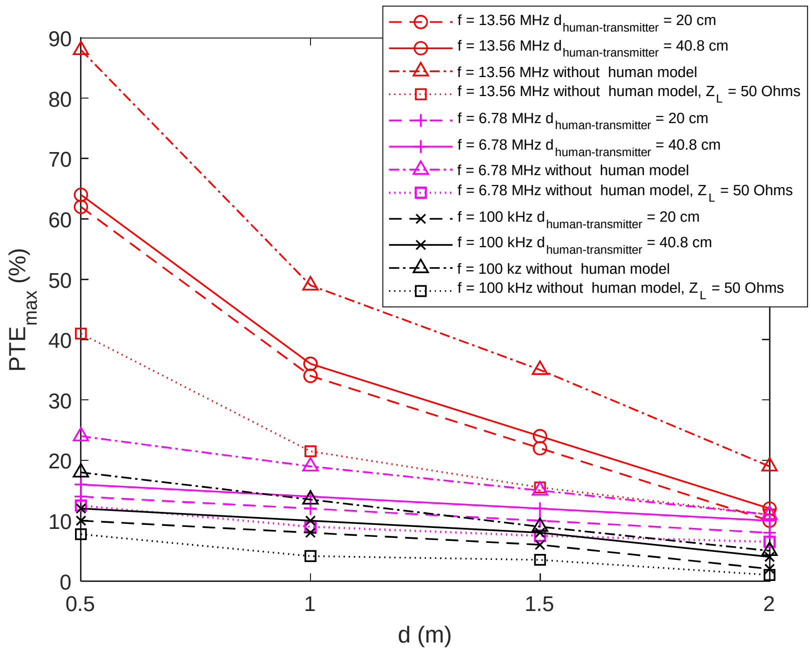

Fig. 5 *PTE_{max} of WPT systems with parallelepiped human model*

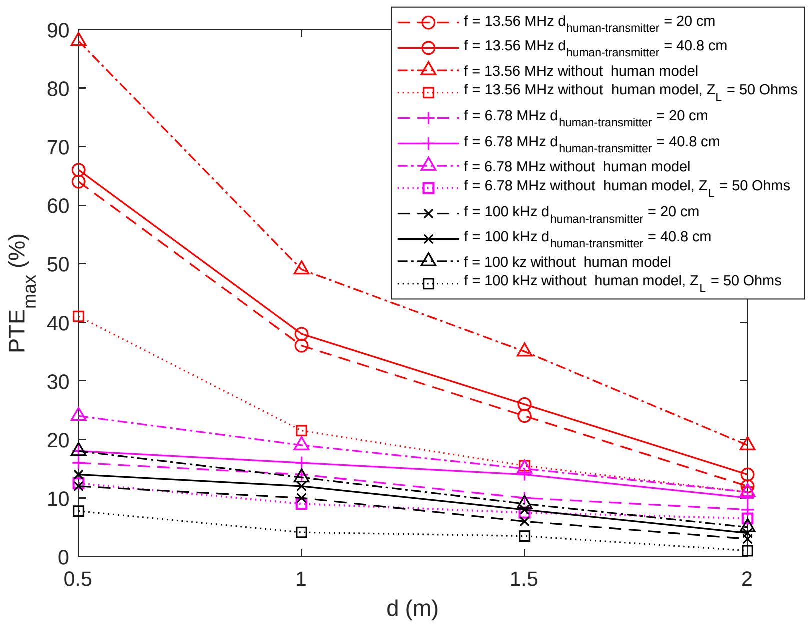

Fig. 6 *PTE_{max} of WPT systems with cylinder human model*

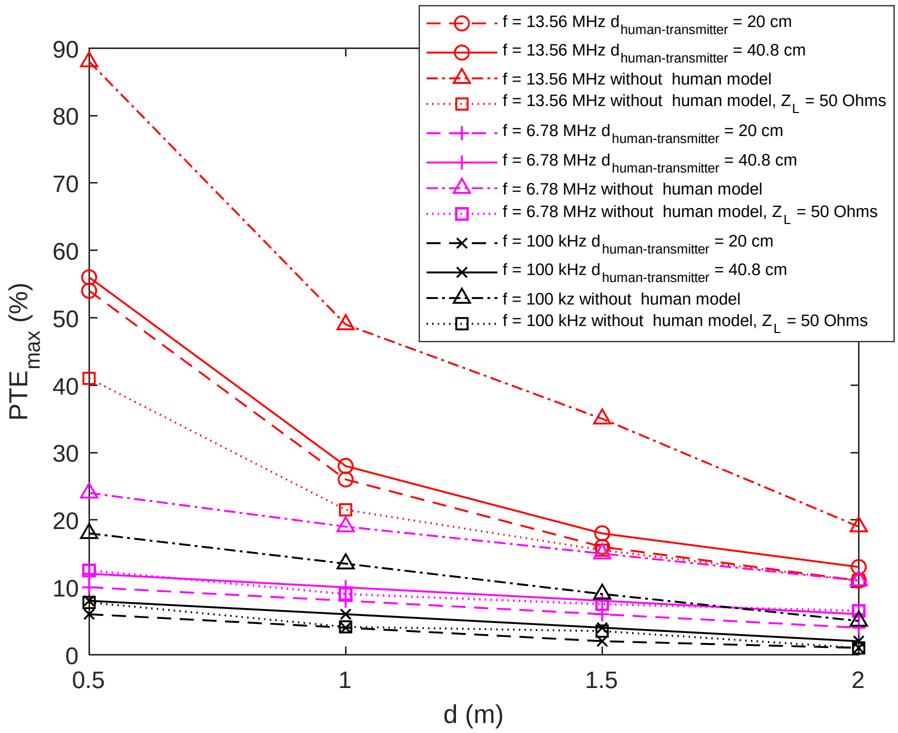

Fig. 7 *PTE_{max} of WPT systems with realistic human model*

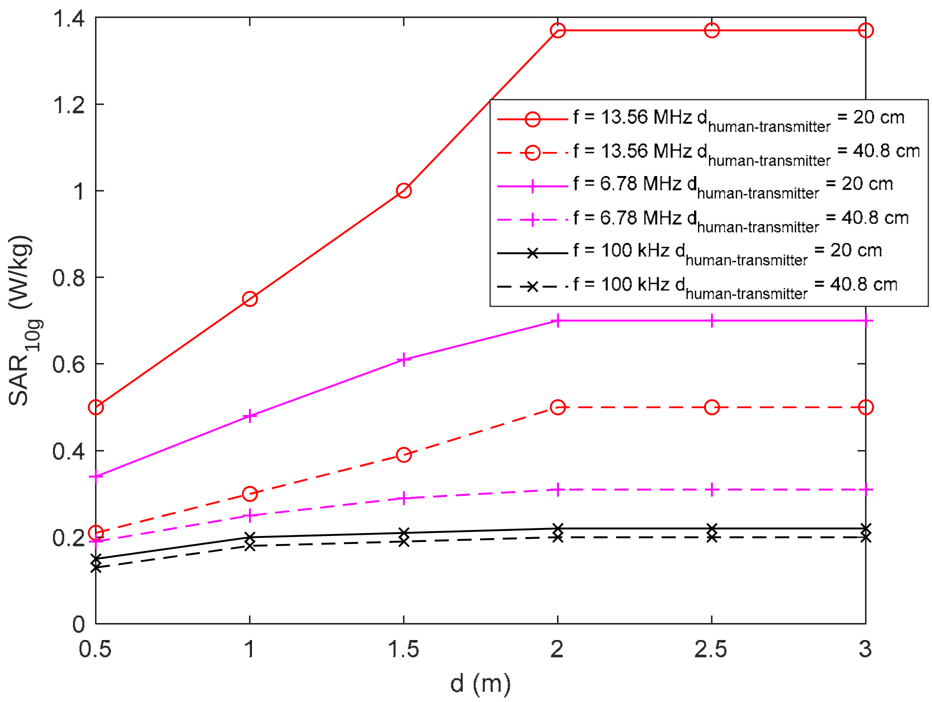

Fig. 8 *SAR_{10g} of WPT systems with parallelepiped human model*

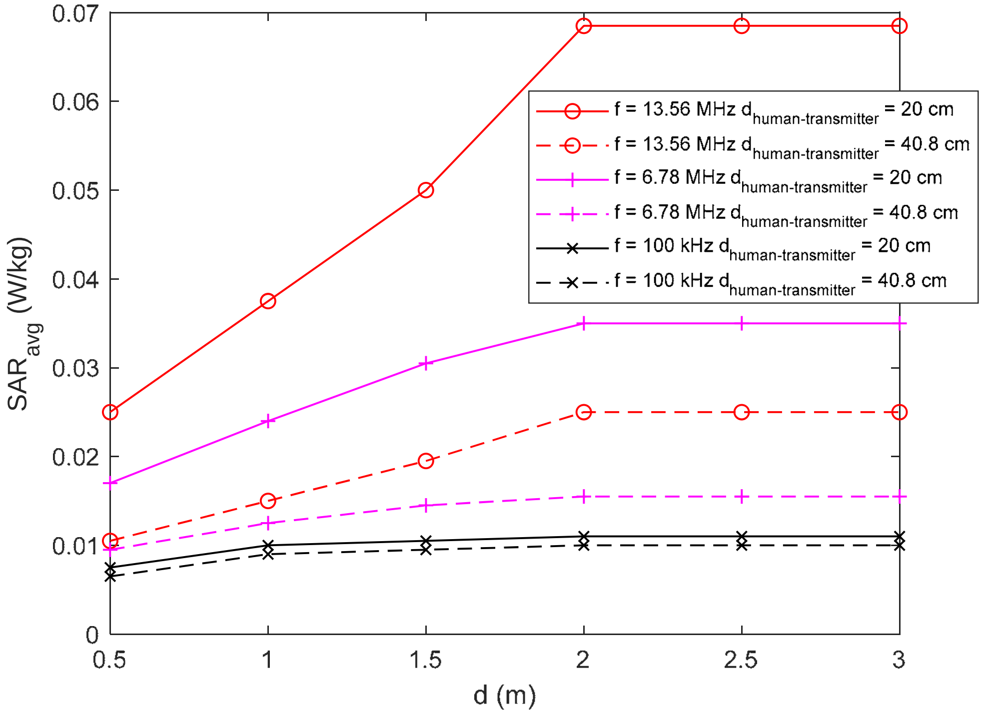

Fig. 9 *SAR_{avg} of WPT systems with parallelepiped human model*

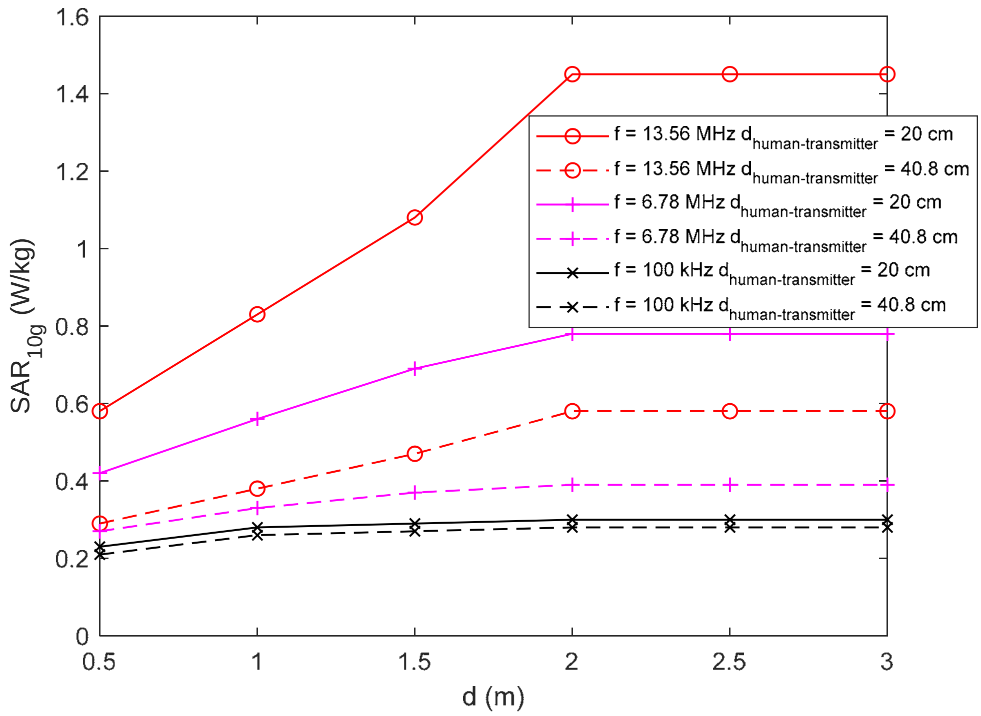

Fig. 10 *SAR_{10g} of WPT systems with cylinder human model*

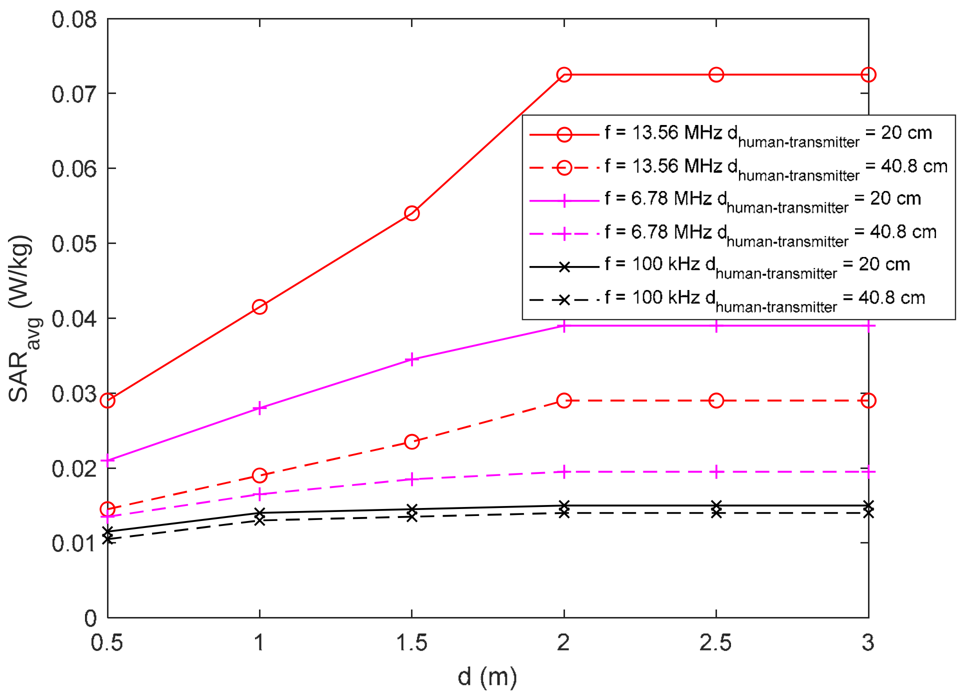

Fig. 11 *SAR_{avg} of WPT systems with cylinder human model*

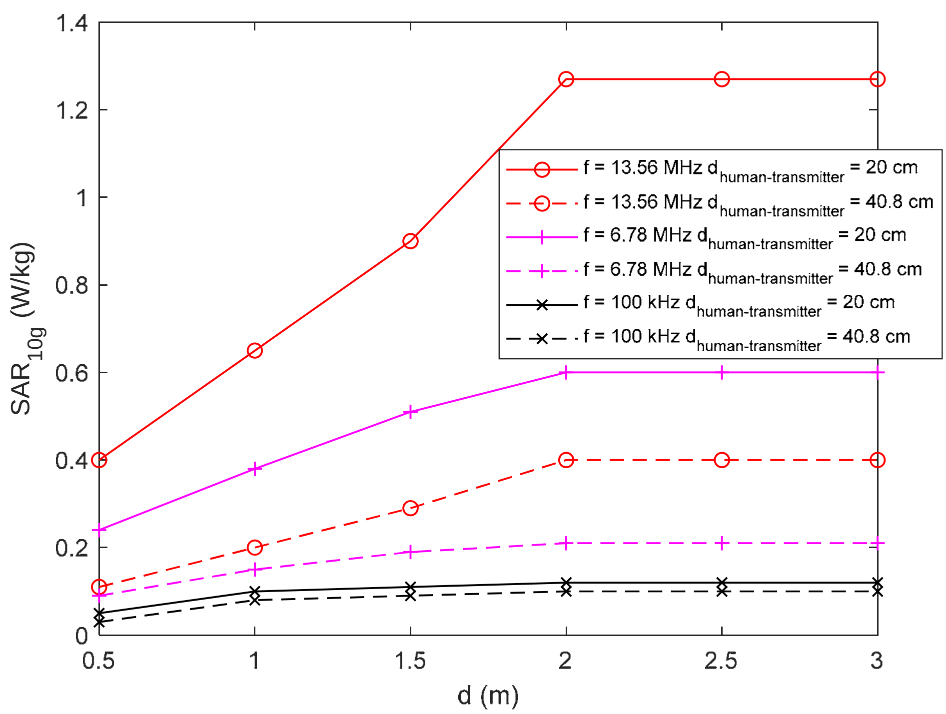

Fig. 12 *SAR_{10g} of WPT systems with realistic human model*

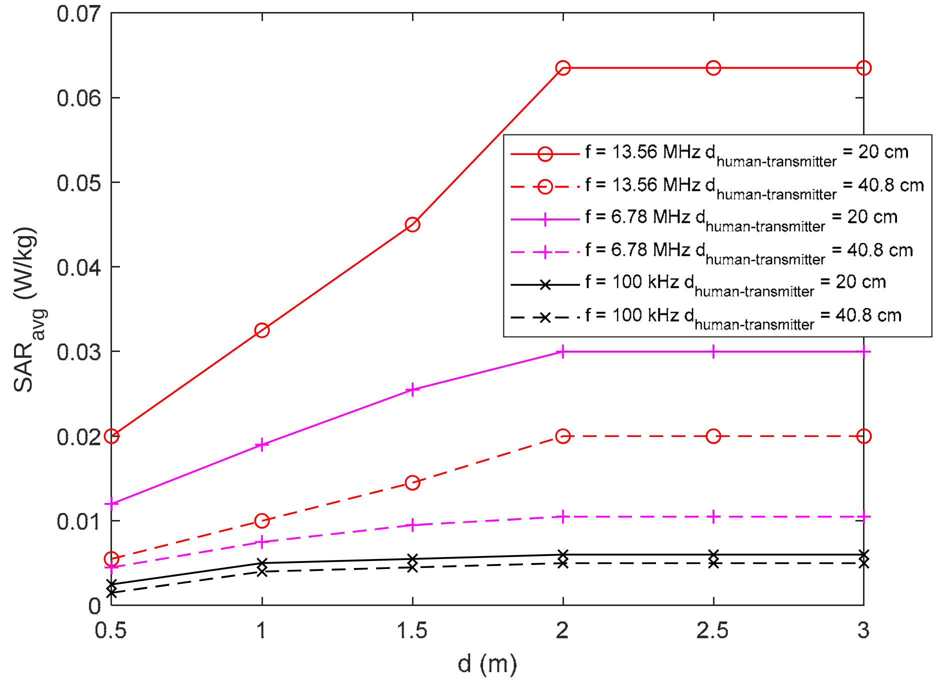

Fig. 13 *SAR_{avg} of WPT systems with realistic human model*

The greatest value of PTE_{max} is obtained without human presence, as expected. Also, for PTE_{max}, the results closest to the realistic human body model result are the ones of the scenario in which the model of a human is parallelepiped. The relative approximation error calculated between simplified and realistic human body model results is on average *+ 12.37 %* for distance $d_{human\text{-}transmitter} = 20$ *cm* and *+ 10.20 %* for $d_{human\text{-}transmitter} = 40.8$ *cm*, shown in Table 5 a) and b). In comparison to realistic a human body model results, slightly different results are found due to the approximation with the simplified model. It is also important to highlight that the equivalence parameter for the simplified and realistic model is the human model height.

The obtained peak SAR_{10g} and SAR_{avg} values are summarized in Table 6. Also, the obtained SAR_{10g} distribution along with the different models of human body (simplified and realistic) at different frequencies is shown in Figures 14–16. The somewhat higher SAR values obtained by simplified models relative to the realistic human model indicate that their use should not lead to the overestimated maximum allowable transmitted power. When the human in the simulation is set closer to the transmitter antenna, SAR_{10g} increases. The conclusion is that SAR_{10g} is smaller when the human moves away from the transmitter antenna toward the receiving one. In any case, the more desirable location of a human is being is closer to the receiver than to the transmitter. The maximum SAR_{10g} is found in the torso, for both models, simplified and realistic. The reason is the almost same dimensions of the torso for the simplified and realistic model and of course, transmitter and receiver antennas are set in front and back of the human model, respectively.

First, one can notice good agreement of the SAR_{10g} and PTE_{max} results for simplified and realistic human body models in FEKO. Then, the PTE_{max} is decreased in all cases where the human model, both simplified or realistic, is present especially for the minimum observed distance $d = 0.5$ *m*, measured from the center of the receiver and center of the transmitter antenna. This is expected because the antenna characteristics are more degraded when the human model is closer. The comparison between WPT systems at different frequencies shows how their fundamental differences influence the PTE_{max} in free space as well as in the presence of the human body model. At the distance d = 1 cm WPT system without human presence at f = *13.56 MHz* obtains *35 %* higher PTE_{max} than WPT system at f = *100 kHz* in free space. Moreover, in the presence of a human body model at d = *2 m*, the WPT system at f = *100 kHz* becomes unusable due to the very low PTE_{max} between the spirals.

Figure 17 and Figure 18 depict scatter diagrams of PTE_{max} and SAR_{10g}, and PTE_{max} and SAR_{avg}, respectively, for equivalent parallelepiped, cylinder and realistic human body models present in different WPT systems and grouped by frequencies. Correlation coefficients r of *−0.445* and *-0.655* for the frequencies f = *13.56 MHz* and f = *6.78 MHz*, respectively, calculated for PTE_{max} and SAR_{10g} results for each case ($d_{human\text{-}transmitter}$ = *20 cm* and $d_{human\text{-}transmitter}$ = *40.8 cm* in front of spiral and square loop WPT system, respectively) confirm that noticeable negative correlation exists between these parameters which means, when PTE_{max} increases, SAR_{10g} decreases. Also, correlation coefficients r of *−0.495* and *-0.683* for the frequencies f = *13.56 MHz* and f = *6.78 MHz*, respectively, calculated for PTE_{max} and SAR_{avg} results for each case ($d_{human\text{-}transmitter}$ = *20 cm* and $d_{human\text{-}transmitter}$ = *40.8 cm* in front of spiral and square loop WPT system, respectively) confirm that noticeable negative correlation exists between these parameters which means, when PTE_{max} increases, SAR_{avg} decreases. This is in agreement to the results of [2] for the frequency f = *13.56 MHz* and spiral WPT system. For the f = *100 kHz* correlation factors are *0.178* and *0.189*, calculated for PTE_{max} and SAR_{10g}, and for PTE_{max} and SAR_{avg}, respectively, for each case ($d_{human\text{-}transmitter}$ = *20 cm* and $d_{human\text{-}transmitter}$ = *40.8 cm* in front of spiral WPT system) indicating scarce or even no correlation between PTE_{max} and SAR_{10g}, and PTE_{max} and SAR_{avg}. From diagrams shown in Figures 15 and 16 it is visible that when PTE_{max} increases, SAR_{10g} and SAR_{avg} decrease. This is probably due to the small antenna efficiency and weaker coupling between spirals at lower frequencies than in other considered cases.

Table 5. *PTE_{max} for different exposure scenarios*

a)

Peak value PTE_{max} (%) at $d_{human\text{-}transmitter}$ = 20 cm			
Type of human model	*f = 13.56 MHz*	*f = 6.78 MHz*	*f = 100 kHz*
Parallelopiped model	*62.512*	*14.497*	*11.128*
Cylinder model	*63.155*	*15.999*	*14.201*
Realistic model	*55.125*	*12.993*	*9.372*

b)

Peak value PTE_{max} (%) at $d_{human\text{-}transmitter}$ = 40.8 cm			
Type of human model	*f = 13.56 MHz*	*f = 6.78 MHz*	*f = 100 kHz*
Parallelopiped model	*64.124*	*16.271*	*13.251*
Cylinder model	*65.897*	*17.769*	*16.877*
Realistic model	*57.476*	*14.227*	*11.653*

Table 6. *Human exposure to the WPT system with a total input power of 5 W*

(a)

Peak value SAR_{10g} (W/kg) at f = 13.56 MHz		
Type of human model	*$d_{human\text{-}transmitter}$ = 20 cm*	*$d_{human\text{-}transmitter}$ = 40.8 cm*
Parallelopiped model	*1.377*	*0.499*
Cylinder model	*1.401*	*0.512*
Realistic model	*1.223*	*0.358*

(b)

Peak value SAR_{10g} (W/kg) at f = 6.78 MHz		
Type of human model	*$d_{human\text{-}transmitter}$ = 20 cm*	*$d_{human\text{-}transmitter}$ = 40.8 cm*
Parallelopiped model	*0.681*	*0.299*
Cylinder model	*0.718*	*0.371*
Realistic model	*0.497*	*0.197*

(c)

Peak value SAR_{10g} (W/kg) at f = 100 kHz		
Type of human model	*$d_{human\text{-}transmitter}$ = 20 cm*	*$d_{human\text{-}transmitter}$ = 40.8 cm*
Parallelopiped model	*0.199*	*0.187*
Cylinder model	*0.255*	*0.232*
Realistic model	*0.155*	*0.122*

(d)

Peak value SAR_{avg} (W/kg) at f = 13.56 MHz		
Type of human model	*$d_{human\text{-}transmitter}$ = 20 cm*	*$d_{human\text{-}transmitter}$ = 40.8 cm*
Parallelopiped model	*0.069*	*0.022*
Cylinder model	*0.071*	*0.029*
Realistic model	*0.064*	*0.019*

(e)

Peak value SAR_{avg} (W/kg) at f = 6.78 MHz		
Type of human model	*$d_{human\text{-}transmitter}$ = 20 cm*	*$d_{human\text{-}transmitter}$ = 40.8 cm*
Parallelopiped model	*0.031*	*0.015*
Cylinder model	*0.038*	*0.019*
Realistic model	*0.025*	*0.009*

(f)

Peak value SAR_{avg} (W/kg) at f = 100 kHz		
Type of human model	*$d_{human\text{-}transmitter}$ = 20 cm*	*$d_{human\text{-}transmitter}$ = 40.8 cm*
Parallelopiped model	*0.009*	*0.007*
Cylinder model	*0.011*	*0.009*
Realistic model	*0.005*	*0.004*

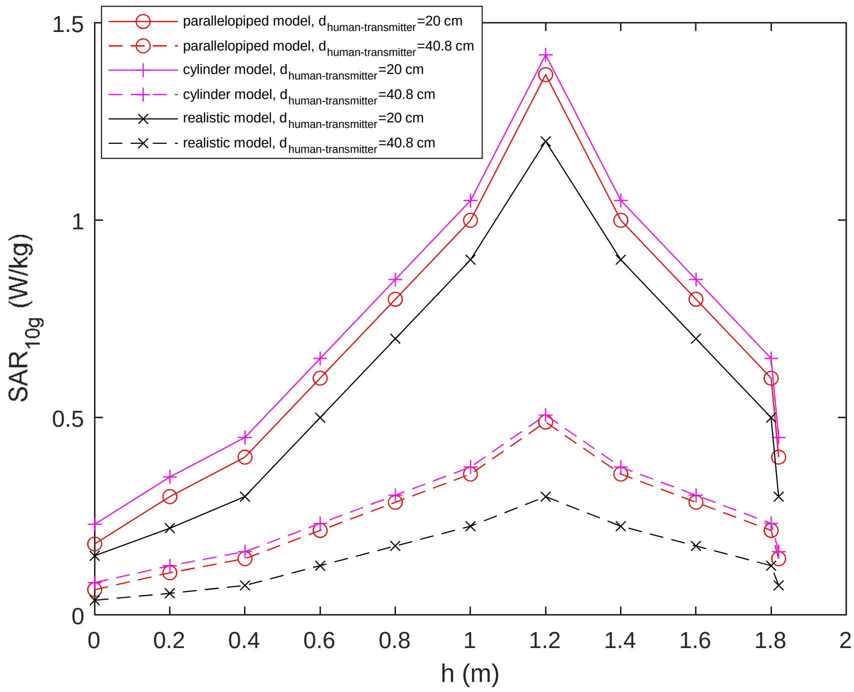

Fig. 14 *SAR_{10g} distribution along the different human body models at f = 13.56 MHz*

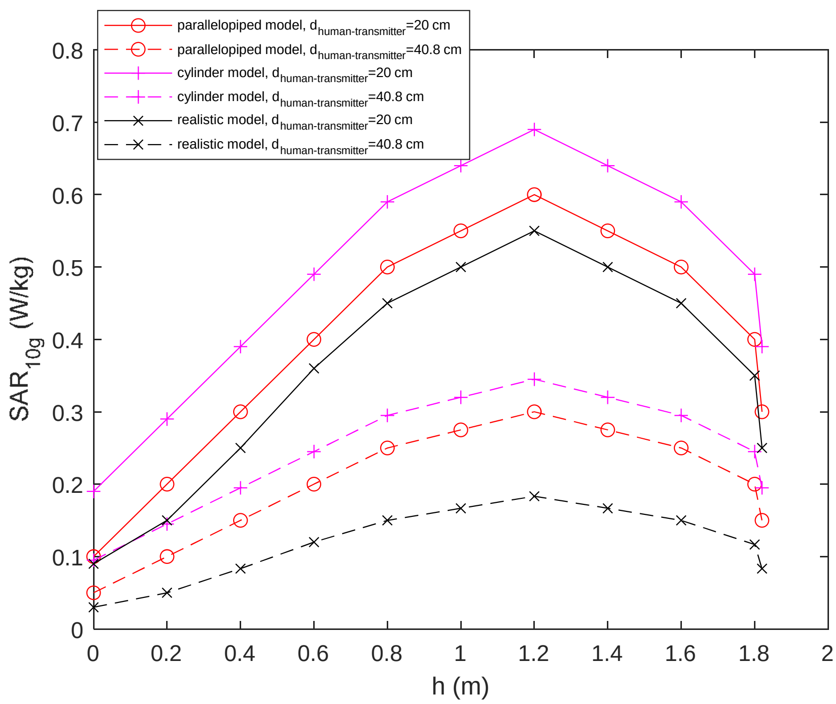

Fig. 15 *SAR_{10g} distribution along the different human body models at f = 6.78 MHz*

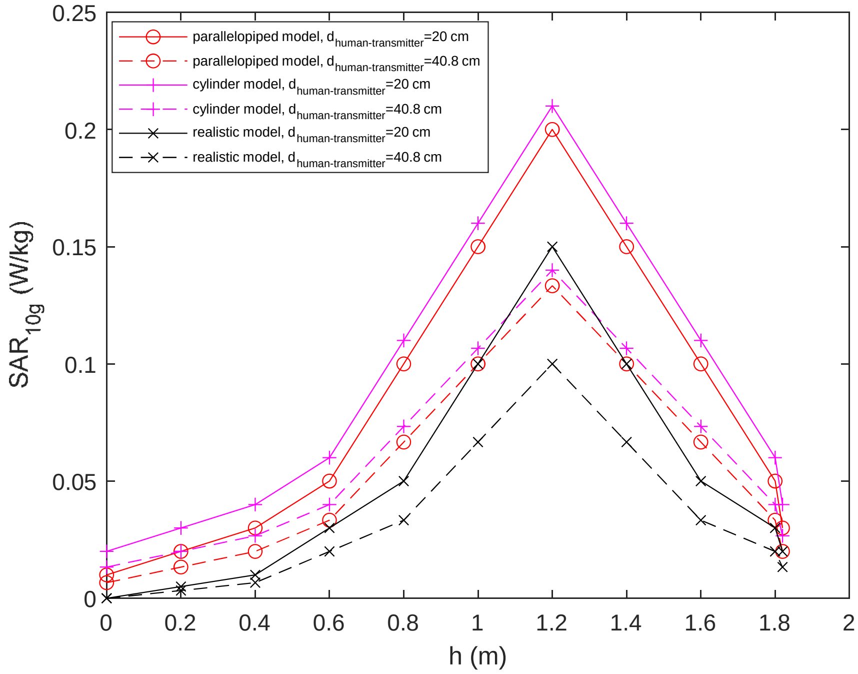

Fig. 16 *SAR_{10g} distribution along the different human body models at f = 100 kHz*

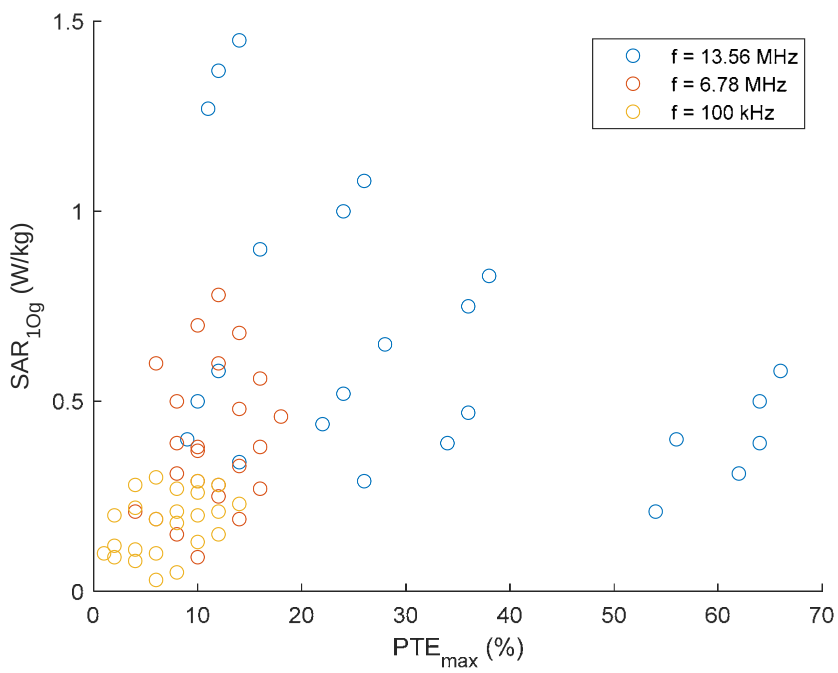

Fig. 17 *Scatter diagram of PTE_{max} and SAR_{10g}*

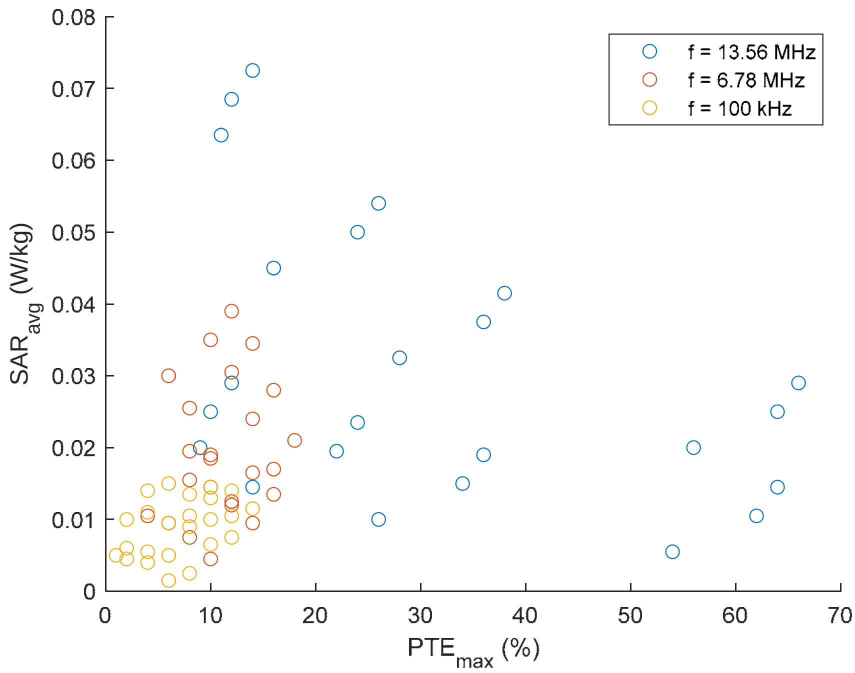

Fig. 18 *Scatter diagram of PTE_{max} and SAR_{avg}*

4. CONCLUSION

In this paper, PTE between two planar antennas at different distances and different frequency bands is simulated. Then, between these two antennas, representing the transmitter and receiving antenna, a simplified human model, a cylinder and a parallelepiped are placed and SAR_{10g} and average SAR values are obtained by numerical calculations. Equivalence of the human model encompasses the assumption that the height and width of that model correspond to the height and width of the average man, respectively. The aim was to show whether simplified human body models such as cylinder and parallelepiped, can be used to simulate human exposure to HF and LF fields. The results of the simulations are compared to the realistic human body model results, as well as to the SAR values that have been prescribed by international guidelines. Conjugate matching is very important to increase system efficiency and deliver maximum energy with as little loss as possible. The simulations performed for two distances from the transmitter indicate that simplified models of the human body can be used for different exposure scenarios at higher frequencies. Their main advantage is a quicker and easier collection of the results. For all examined models in interaction with LF and HF WPT systems, it is shown that the SAR_{10g} and average SAR do not exceed the limits prescribed by international guidelines for this 5-W WPT system scenario. The noted small differences between simulated SAR scenarios are most likely because of the different volumes of models and/or slightly different gaps between human and WPT system antennas. It is shown that there is no significant difference between SAR and PTE_{max} while using simplified models in defined scenarios (antennas near torso) which proves the usefulness for theoretical calculations of human body exposure limited to the simplified models. But, when antennas are put near neck or knees (because of difference in dimensions of specified areas in simplified and realistic models) there is a slight difference in results so in that scenario usage of simplified model is limited and realistic model is a better alternative for theoretical calculations.

5. LITERATURE

[1] Y. Tak, J. Park, S. Nam, The optimum frequency for near-field coupled small antennas, *IEEE Trans. Antennas Propag.*, Vol. 59, No. 3, pp. 1027-1031, 2011.

https://doi.org/10.1109/TAP.2010.2103034

[2] M. Škiljo, Z. Blažević, D. Poljak, Interaction between humans and near-field of wireless power transfer systems, Progress In Electromagnetics Research C, Vol. 67, pp. 1–10, 2016. https://doi.org/10.2528/PIERC16062005

[3] D. Poljak, Human exposure to non-ionizing radiation, Kigen, Zagreb, 2006.

[4] IEEE Standard for Safety Levels with Respect to Human Exposure to Radio Frequency Electromagnetic Fields, 3 kHz to 300 GHz, C95, 1-2005 (New York: IEEE)

[5] H.A. Wheeler, The spherical coil as an inductor, shield, or antenna, Proc. IRE, Vol. 46, No. 9, pp. 1595-1602, 1958. https://doi.org/10.1109/JRPROC.1958.286978

[6] L.J. Chu, Physical limitations of omni-directional antennas, *Journal of Applied Physics*, Vol. 19, pp. 1163-1175, 1948. https://doi.org/10.1063/1.1715038

[7] W. Wasylkiwskyj, W.K. Kahn, Scattering properties and mutual coupling of antennas with prescribed radiation pattern, *IEEE Trans. Antennas Propag.*, Vol. AP-18, No. 6, pp. 741-752, 1970. https://doi.org/10.1109/TAP.1970.1139795

[8] C.A. Balanis, *Antenna Theory: Analysis and Design*, 2nd ed., John Wiley & Sons, Inc., USA, 1997.

[9] P. Hasgall, E. Neufeld, M. Gosselin, E. Neufeld, ITIS Database for thermal and electromagnetic parameters of biological tissues, 2011.

[10] A. Chiba, K. Isaka, Y. Yakoi, M. Nagata, K. Kitagav, T. Matsuo, Application of the Finite Element Method to Analysis of Induced Current Densities Inside Human Model Exposed to 60 Hz Electric Field, *IEEE Trans Power Apparatus and Systems*, Vol. PAS-103, No. 7, pp 1895-1901, July 1984. https://doi.org/10.1109/TPAS.1984.318655

[11] A. Chiba, K. Isaka, Y. Onogi, Analysis of Current Densities Induced Inside Human Model Exposed to AC Electric Field, *Electronics and Communication in Japan*, Part 2, Vol. 79, No. 4, 1994.

[12] A. Chiba, K. Isaka, Y. Onogi, Analysis of Current Densities Induced Inside Human Model by the Two-Steps Process method Combining the Surface Integral Equation and the Finite Element Method, *Electronics and Communication in Japan*, Part 2, Vol. 79, No. 4, 1994. https://doi.org/10.1002/ecjb.4420790412

[13] C. Gonzales, A. Peratta, D. Poljak, Boundary element modeling of the realistic human body exposed to extremely low frequency (elf) electric fields: Computational and geometrical aspects, *IEEE Trans. On EMC*, Vol. 49, No. 1, pp. 153-62, 2007.

https://doi.org/10.1109/TEMC.2006.888167

[14] C. Gonzalez, A. Peratta, D. Poljak, Induced Currents in the human body resulting from the proximity to surfaces at fixed potentials, *Proceedings SoftCOM 2007*/Split: FESB, pp. 139-143, 2007. https://doi.org/10.1109/SOFTCOM.2007.4446080

[15] C. Gonzalez, A. Peratta, D. Poljak, Human body exposure to fixed potential surfaces in power substations, *Modelling in Medicine and Biology VII*/Brebbia, Carlos A. (ur.). Southampton: WIT Press, pp. 243-252, 2007. https://doi.org/10.2495/BIO070241

[16] D. Čavka, D. Poljak, A. Peratta, C. Brebbia, Boundary element model of the human head exposed to electrostatic field generated by Video Display Units, Boundary Elements and Other Mesh Reduction Method/Škerget, L., Brebbia, C.A., Southampton: WIT Press, pp. 115-124, 2008. https://doi.org/10.2495/BE080121

[17] C. Gonzalez, A. Peratta, D. Poljak, Pregnant women exposed to extremely low frequency electromagnetic fields, *Proceedings of 2008 International Conference on Software, Telecommunications and Computer Networks*/Rožić, Split: FESB, 2008.

https://doi.org/10.1109/SOFTCOM.2008.4669443

[18] C. Gonzalez, A. Peratta, D. Poljak, Electromagnetic modeling of fetus and pregnant women exposed to extremely low frequency electromagnetic fields, *Boundary Elements and Other Mesh Reduction Methods XXX/Southampton:* WIT Press, pp. 85-94, 2008.

https://doi.org/10.2495/BE080091

[19] O.P. Gandhi, Some Numerical Methods for Dosimetry: Extremely Low Frequencies to Microwave Frequencies, *Radio Sci*., Vol. 30, No. 1, pp. 161-177, Jan-Feb. 1995.

https://doi.org/10.1029/94RS01158

[20] O.P. Gandhi, J.Y. Chen, Numerical Dosimetry at Power Line Frequencies Using Anatomically Based Models, *Bioelectromagnetics Suppl*., Vol. 1, pp. 43-60, 1992.

https://doi.org/10.1002/bem.2250130706

[21] O.P. Gandhi, Y. Gu, Y.J.Y. Chen, H.I. Bassen, Specific Absorption Rates and Induced Current Distributions in an Anatomically Based Model for Plane Wave Exposures, *Health Physics*, Vol. 63, No. 3, pp. 281-290, Sept. 1992.

https://doi.org/10.1097/00004032-199209000-00003

[22] T.W. Dawson. K. Caputa, M.A. Stuchly, High-Resolution Organ Dosimetry for Human Exposure to Low Frequency Electric Fields, *IEEE Trans. Power Delivery*, Vol. 13, No. 2, pp. 366-373, April 1998. https://doi.org/10.1109/61.660903

[23] R. Tseng, B. von Novak, S. Shevde, K.A. Grajski, Introduction to the alliance for wireless power loosely-coupled wireless power transfer system specification version 1.0, 2013 *IEEE Wireless Power Transfer* (WPT), Perugia, pp. 79-83, 2013.

https://doi.org/10.1109/WPT.2013.6556887

[24] D. Rubin, The Linville method of high frequency transistor amplifier design, Naval Weapons Center, Research Department, NWCCL TP 845, Corona Laboratories, Corona, California, March 1969.[25] IT'IS Database, from Internet: http://www.itis.ethz.ch/virtual-population/tissue-properties/database/dielectric-properties